IEEE Journal of Translational Engineering in Health and Medicine

Received 3 December 2018; revised 8 April 2019 and 21 April 2019; accepted 6 May 2019. Date of publication 4 June 2019; date of current version 18 June 2019.

Digital Object Identifier 10.1109/JTEHM.2019.2919020

Reduced Rank Least Squares for Real-Time Short Term Estimation of Mean Arterial Blood Pressure in Septic Patients Receiving Norepinephrine

YI TANG[1], SAMUEL BROWN[2,3], JEFF SORENSEN[3], AND JOEL B. HARLEY[1,4], (Member, IEEE)

[1]Department of Electrical and Computer Engineering, The University of Utah, Salt Lake City, UT 84112, USA
[2]Department of Pulmonary and Critical Care, School of Medicine, University of Utah, Salt Lake City, UT 84132, USA
[3]Department of Pulmonary and Critical Care, Intermountain Medical Center, Murray, UT 84107, USA
[4]Department of Electrical and Computer Engineering, University of Florida, Gainesville, FL 32603, USA

Corresponding author: J. B. HARLEY (joel.harley@ufl.edu)

This work was supported in part by the National Institute of General Medical Sciences under Grant 1K23GM094465 to SMB, in part by the Intermountain Research and Medical Foundation, and in part by the Easton Fund.

ABSTRACT Norepinephrine (NE), an endogenous catecholamine, is a mainstay treatment for septic shock, which is a life-threatening manifestation of severe infection. NE counteracts the loss in blood pressure associated with septic shock. However, an NE infusion that is too low fails to counteract the blood pressure drop, and an NE infusion that is too high can cause a hypertensive crisis and heart attack. Ideally, the NE infusion rate should maintain a patient's mean arterial blood pressure (MAP) above 65 mmHg. There are a few data-driven, quantitative models to predict the MAP, and incorporate NE effects. This paper presents a model, driven by intensive care unit (ICU) measurable data and known NE inputs, to predict the future MAP of an ICU patient. We derive a least square estimation model for MAP based on available ICU data, including heart period, NE infusion rate, and respiration wave. We learn the parameters of our model from initial patient data and then use this information to predict future MAP data. We assess our model with data from 12 septic patients. Our model successfully predicts and tracks MAP when the NE infusion rate changes. Specifically, we predict MAP 3 to 20 min in the future with the mean error of less than 4 to 7 mmHg over 12 patients. *Conclusion:* this new approach creates the potential to advance methods for predicting NE infusion rate in septic patients. *Significance:* successfully predicted patients' MAP could reduce catastrophic human error and lessen clinicians' workload.

INDEX TERMS Least squares (LS), mean arterial blood pressure (MAP), sepsis, shock, norepinephrine (NE).

I. INTRODUCTION

Vasopressors, most commonly norepinephrine (NE), are widely used to treat septic shock and stabilize hemodynamic variables, such as blood pressure, and decrease the duration of shock. The benefit of using a vasopressor on septic patients is to maintain perfusion of tissues thereby preserving life. Compared with dopamine, another drug commonly used for regulating blood pressure, NE improves the splanchnic tissue oxygen utilization in sepsis [1]. Mean arterial blood pressure (MAP) control in septic patients is typically based on clinician experience. In ICU treatments, nurses and physicians manually adjust the NE infusion rate to ensure that the MAP is within a safe region, often defined as greater than 65 mmHg and no less than 60 mmHg in some cases [2], [3]. These numbers are recommended by the Surviving Sepsis Campaign Guideline [4]. Due to this guideline, clinicians must check blood pressure frequently and there is a chance of a catastrophic human error. Ultimately, the error could result in death.

As a result, clinicians want an approach to predict the effects of NE, reduce the burden of constant monitoring, and reduce human error. With methods to predict the effects of NE, a new system could titrate NE automatically and could significantly improve a patient's drug response and ensure blood pressures remain in safe regions. Yet, there are currently few methods for accurately estimating MAP

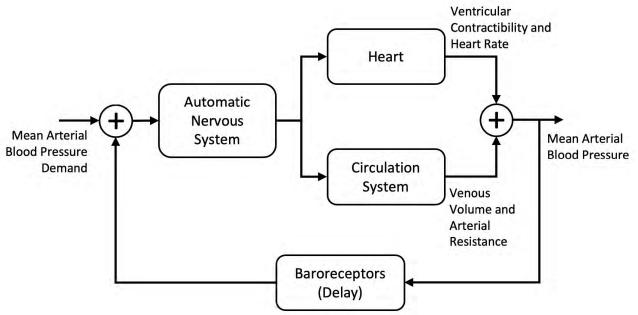

FIGURE 1. **Baroreflex model flow chart.**

based on the current NE infusion rate. Furthermore, there are few dynamic MAP models for patients with septic shock, whose physiology is different from healthy people, making it difficult to create these methods.

A NE-based, dynamic MAP model is needed to control NE infusion rates. In addition to the NE infusion, available ICU data could augment the model and improve our predictive ability. Previous research has defined several physiology MAP models based on ICU data [5], [6], but few accounts for the effects of NE. According to Mukkamala [7], the underlying model for MAP is based on a combination of four components: heart rate, ventricular contractility, systemic venous unstressed volume, and systemic arterial resistance. These components are illustrated in Fig 1. In this model, each component is nonlinearly adjusted by the autonomic nervous system (ANS), which is a biological control system in humans and animals, based on the history of the differences between the detected blood pressure and the ANS expected blood pressure. Yet, this is an ideal model and requires data that is typically immeasurable from the patient.

In general, a clear pharmacodynamics model of NE's effect on MAP has not been determined from previous studies [8]. Based on prior work, NE is metabolized by intracellular enzymes [9] and mainly eliminated by the liver [10] as well as kidney. According to Beloeil's study of septic patients [8], the kinetics of NE fits a first-order elimination linear one-compartment model, and other research [11] confirms that the norepinephrine plasma levels of NE are predictable. However, just knowing the pharmacodynamics model of NE is not sufficient because the pharmacodynamics of NE are not yet clear. In other words, the relationship between the concentration of NE and MAP is relatively unknown. In addition, the NE concentration level is not accessible in real time in the ICU environment, only the current infusion rate. Beloeil *et al.* [8] and Kamendi *et al.* [12] have created a NE pharmacodynamics model based on a sigmoidal Emax model, which is a common nonlinear pharmacodynamics model based on knowing the maximum effect attributable to the drug. However, the required parameters are not commonly available. Yapps [13] statistically predicts hypotension occurrence in sepsis patients with logistic regression but does not specifically predict future MAP values. Furthermore, Zhu [14] proposed a dose-response based NE-MAP model for swine without the consideration of sepsis. Similarly, Bighamian *et al.* [15], [16] introduced a latency-dose-response-cardiovascular model to predict MAP, heart rate, and other cardiovascular parameters under NE but has only verified it in piglets without sepsis.

Neural networks and machine learning have been studied for similar applications [17]. These approaches have not included the effect of NE and are usually best utilized with a large training data set. Merouani *et al.* [18] developed a MAP fuzzy control system for decreasing NE infusion rates in septic shock patients. The system did not formally predict MAP. It was geared toward decreasing NE rather than titrating NE and does not address stability issues. Guinot *et al.* [19], [20] used arterial dynamic elastance, known as Eadyn, to predict the effects of decreasing in norepinephrine infusion rates. Yet the approach does not predict future MAP or provide estimates to predict the effect of increasing the norepinephrine infusion rate.

As a result, there is a need to build a model that can successfully relate NE and sepsis to MAP with available ICU data in septic patients. This paper focuses on creating this model for septic patients under known NE infusions rates. Our work combines medical and engineering knowledge on MAP control in a clinical environment. We use a reduced-rank least squares (LS) model with multiple inputs commonly acquired in the ICU, including heart rate, respiration wave, and NE infusion rate. We train and test our model with data from twelve patients treated at the Shock Trauma ICU at the Intermountain Medical Center in Murray, Utah. We used the model to predict human MAP during NE infusion. As expected, the prediction error of the model increases as the length of our prediction window increases. The model is able to reach 6 mmHg root mean squared error (RMSE) when predicting 10 mins into the future and 7.5 mmHg when predicting 20 mins into the future.

II. METHODS

We model MAP as a time-varying, linear system with multiple time series inputs. The linear model assumes that the output of the system can be represented by a linear combination of the output's previous values, the current inputs, and the previous inputs. This model is similar to a digital filter [21] or neural network [22] model. We use this model since it has been shown that MAP can be expressed as the convolution of its previous values [7]. Our inputs include the heart rate, respiratory wave, and NE infusion rate.

Our model is trained and adapts based on the status of a single patient. Therefore, the model is time-varying and patient-specific. Adaptation is necessary for several reasons. First, MAP is a function of NE infusion rate. That is, a higher NE infusion increases the MAP. Yet, the rate that MAP increases is generally slow [8] and varies between patients [8]. Practitioners currently wait approximately 3-15 minutes before the adjustment of the NE rate. Furthermore, since the septic patient's baroreflex system does not function normally, its relationship with MAP is difficult to predict and is

IEEE Journal of Translational Engineering in Health and Medicine

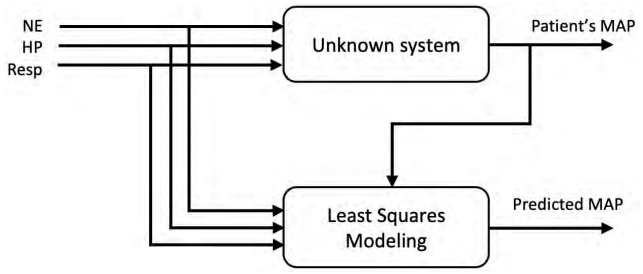

FIGURE 2. **Baroreflex modeling flow chart.**

inherently time-varying. The ability to adaptively train a linear model allows our method to learn not only the status of patients but also predict the effects of NE at a given moment in time.

In this section, we formulate our east squares model and its implementation. Specifically, we describe our approach for preprocessing the data followed by learning and applying the model to optimally predict patient MAP. Our process is demonstrated by the flow chart shown in Figure 2. In this paper, the unknown system is a septic patient's baroreflex system. Once the model is known, we can use it with current and past measurements to predict future data.

A. SETTING

The patients studied were admitted to the 24-bed Shock Trauma ICU or the 12-bed Respiratory ICU at Intermountain Medical Center, an academic hospital in Murray, Utah, USA. This study was approved by Intermountain's Institutional Review Board (#1020798) with a waiver of informed consent.

B. DATA COLLECTION

In our model, we predict future MAP based on common ICU measurements: the NE infusion rate per unit weight, the patient's heart period, and the patient's respiratory pattern. Table 1 describes each of these parameters and their units. In a clinical setting, the MAP, the NE infusion rate, and the patient's heart period can be computed directly from measurements taken by ICU equipment. Specifically, the MAP and respiration wave is calculated from the arterial blood pressure (ABP) waveform, which is recorded by standard ICU monitors. The NE infusion rate is recorded by the infusion pump in the ICU and is automatically uploaded to our electronic medical record system in our hospital by the infusion pumps via the wireless network. Instead of using heart rate, we measure the heart period (HP) by calculating the time interval between each heart beat. The respiration wave is a measure of respiratory function and is a key input into the parasympathetic arm of the autonomic nervous system. It is measured by computing the wave of the diastolic end of the arterial blood pressure (i.e., valley envelope of the arterial blood pressure). In a real-time clinical setting, the envelope is computed by smoothing the diastolic square wave. The diastolic wave is captured by taking the diastolic signal of previous heart period.

TABLE 1. **Data parameter characteristics.**

Parameters	Characteristics	Unit
MAP	Mean arterial blood pressure: calculated by taking the mean of arterial blood pressure within each heartbeat	mmHg
HP	Heart Period: time interval between each heartbeat	second
NE	Norepinephrine equivalent infusion rate	mg/(minkg)
Resp	Respiratory wave: inferred from smoothed diastolic wave	mmHg

Based on the results in the literature [7], our model assumes that the MAP can be predicted from time-variations in these four inputs. Figure 3 illustrates these inputs from one example septic patient. In this figure, we observe that NE changes more often during the first half of the dataset to stabilize the patient's hemodynamic status early. Commonly, the NE is titrated to maintain a MAP of 60-70 mmHg.

Note that while the data can be effectively gathered from the ICU equipment, much of the data is corrupted by noise. Most noise in the patient data is the result of physical movement by the patient or from clinicians handling the ICU equipment. In one typical patient, for example, the standard deviation of MAP in a 1-hour window across an 11-hour period varies from 1.19 mmHg to 20.7 mmHg.

C. PREPROCESSING AND SMOOTHING

Factors that contribute to noise cannot be easily controlled and noise can be substantial. Therefore, noise reduction is an important preprocessing step before learning the LS model. Periods of high noise are manually eliminated by connecting the data before and after noise. These periods usually start with a large spike that is followed by unrealistically large constant values (> 90 mmHg), or constant values (< 40 mmHg), or large, rapid variations (> 5 mmHg variations between successive heart beats).

Noise reduction is then applied on periods of relatively lower noise by averaging the data over time. Specifically, we use a real-time single-pole averaging filter to average noise. These filters are commonly used in noise reduction applications, including audio noise reduction [23]. The output $y(n)$ of a single-pole filter is defined by

$$y(n) = \beta y(n-1) + (1-\beta)x(n) \tag{1}$$

where $x(n)$ represents any patient input data (MAP, heart period, or the respiration wave), $y(n)$ represents filtered data, and β is the filtering coefficient. A large value (near one) of β corresponds to a high degree of smoothing while low values (near zero) correspond to little smoothing. We apply this single-pole filter to each of our four inputs. In this paper, we use a filtering coefficient of 0.9999 to achieve a long smoothing operation. The equivalent time constant of this smoothing filter is 79.992 seconds.

Figure 3 illustrates the inputs after applying smoothing. Note that we also apply smoothing to the NE input since it is reasonable to assume there is a time constant for the change

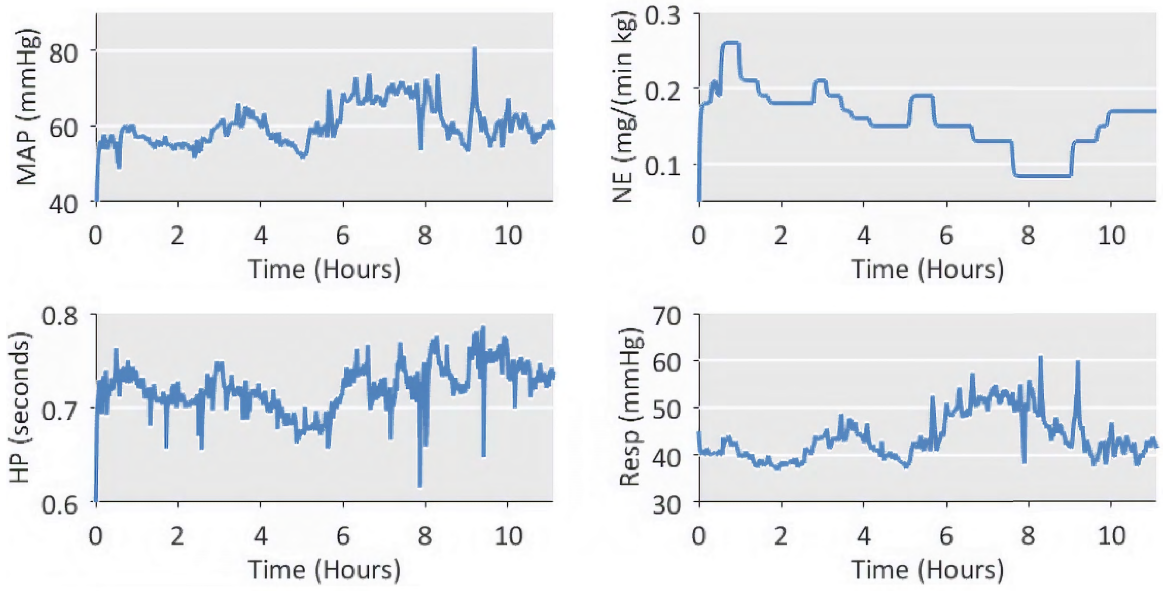

FIGURE 3. The sample plots of observed MAP (top right), NE infusion rate (top left), heart period (bottom left), and captured respiration (bottom right).

in NE input to take effect. In addition, smoothing the input also reduces unrealistic, abrupt changes in our prediction.

D. LEAST SQUARES CARDIOVASCULAR MODEL

In this subsection, we introduce our model for defining the relationship between MAP, NE infusion rate, heart period, and respiration wave. Specifically, the model is defined by

$$\mathbf{x}(n) = \mathbf{A}(n)\mathbf{x}(n-P) \tag{2}$$

where $\mathbf{x}(n)$ is a vector of the last N previous measurements for MAP, NE infusion rate, heart period, and respiration wave. We refer to this as our state vector. We define the state vector $\mathbf{x}(n)$ as

$$\begin{aligned}\mathbf{x}(n) = [&\mathrm{MAP}(n) \cdots \mathrm{MAP}(n-N+1)\ \mathrm{HP}(n) \\ &\cdots \mathrm{HP}(n-N+1)\ \mathrm{NE}(n) \cdots \mathrm{NE}(n-N+1) \\ &\times \mathrm{Resp}(n) \cdots \mathrm{Resp}(n-N+1)]\end{aligned} \tag{3}$$

The matrix $\mathbf{A}(n)$ represents weights that relate prior states from P time-samples in the past to the current states. That is, we assume the last N inputs and outputs can be represented by a linear combination of the N last states from P time-samples previous. Based on this model, the weight matrix $\mathbf{A}(n)$ needs to be learned through system identification.

E. REDUCED RANK MODEL LEARNING

To learn our model, we determine the relationship between the previous states and the current states. It should be noted that there are $4N \times 1$ current and past states and $4N \times 4N$ weights in $\mathbf{A}(n)$ to learn. For one collection of states, this represents a highly underdetermined problem. Therefore, we learn $\mathbf{A}(n)$ from a collection of states across different points in time. We achieve this by building an $4N \times D$ Toeplitz matrix of data

$$\mathbf{X}(n) = [\mathbf{x}(n)\ \mathbf{x}(n-1)\ \cdots\ \mathbf{x}(n-D+1)] \tag{4}$$

so that we can now represent our model as

$$\mathbf{X}(n) = \mathbf{A}(n)\mathbf{X}(n-P)\ . \tag{5}$$

Compared with our previous expression in (2), this model assumes that the relationship $\mathbf{A}(n)$ between the current and past states is constant during the last D time samples. For this paper, we use $D = 6000$ (20 minutes) of past states to learn $\mathbf{A}(n)$.

Through this formulation, we are able to solve for $\mathbf{A}(n)$ through a standard matrix inversion (assuming $D > 4N$) or least squares inversion. Yet, this approach still has significant challenges. Through the inversion process, an ill-conditioned data matrix $\mathbf{X}(n-P)$ with noise can significantly change our learned weights $\mathbf{A}(n)$ and cause instabilities when predicting future states. Therefore, we perform a least squares matrix inversion through a reduced-rank approximation of the data.

Specifically, we first compute a reduced-rank (i.e., reduced-dimension) approximation of the data matrix $\mathbf{X}(n-P)$ to remove noise that causes instabilities. We compute the singular value decomposition

$$\mathbf{X}(n-P) = \mathbf{U}\mathbf{S}\mathbf{V}^T, \tag{6}$$

which decomposes $\mathbf{X}(n-P)$ into two orthogonal singular vector matrices $\mathbf{U}$ and $\mathbf{V}$ and one diagonal singular value matrix $\mathbf{S}$. We then remove rows and columns of $\mathbf{U}$, $\mathbf{V}$ and $\mathbf{S}$ that correspond to singular values that are less than a given threshold τ. This produces smaller matrices $\widehat{\mathbf{U}}$, $\widehat{\mathbf{S}}$, and $\widehat{\mathbf{V}}^T$ that create the reduced-rank approximation

$$\widehat{\mathbf{X}}(n-P) = \widehat{\mathbf{U}}\,\widehat{\mathbf{S}}\,\widehat{\mathbf{V}}^T \tag{7}$$

IEEE Journal of Translational Engineering in Health and Medicine

for the data matrix. In this process, we choose our singular value threshold $\tau = 50$ based on our observations of the singular values.

We learn $\mathbf{A}(n)$ by performing a least squares inversion on the reduced-rank approximation of the data matrix. That is, our estimate of $\mathbf{A}(n)$ is expressed as

$$\widehat{\mathbf{A}}(n) = \left[\widehat{\mathbf{X}}(n-P)\right]^{\dagger} \mathbf{X}(n) \tag{8}$$

where $[\cdot]^{\dagger}$ corresponds to the Moore-Penrose pseudo-inverse operation. The Moore-Penrose pseudo-inverse is equivalent to the least squares inverse solution [2].

F. MODEL PREDICTION

To predict future states, we assume the relationship between the states from P time samples in the past and current states is equivalent to the relationship between the current states and states that are P time samples in the future. Therefore, we can use the weights matrix $\mathbf{A}(n)$ to predict future states. Specifically, we predict future states by computing

$$\widehat{\mathbf{x}}(n+P) = \mathbf{A}(n)\mathbf{x}(n) \tag{9}$$

Note that this approach does not just predict the future MAP. It also predicts the future heart period and respiratory wave. Figure 4 demonstrates the predicted MAP in dark line along with real MAP in light line.

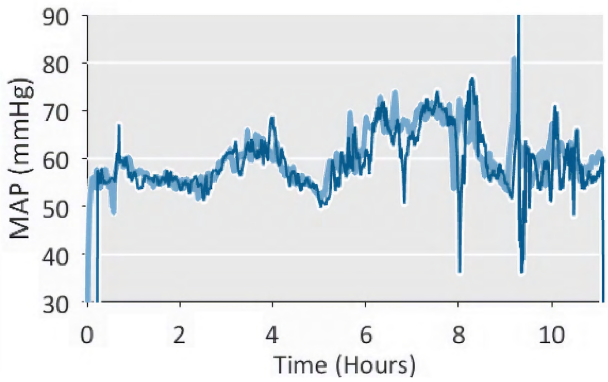

FIGURE 4. A sample prediction period where the light curve represents the true MAP and the dark line represents the predicted MAP.

III. CASE STUDY

A. PATIENT DATA

To demonstrate our approach, we collected ICU data from 103 patients with severe sepsis or septic shock with an indwelling arterial catheter at the Shock Trauma ICU in the Intermountain Medical Center in Murray, Utah. Table 1 displays the parameters collected in this study: the MAP, heart period, respiration wave, and NE equivalent infusion rate. The original data is sampled from bedside Philips Intellivue monitors using the Research Data Export (RDE) functionality. RDE provides 125-Hz digitized tracings of arterial blood pressure and EKG. The NE equivalent infusion rate is sampled at 1 per minute. Due to the difference in the sampling rate of patient's data from the Intermountain Healthcare ICU patients' database, we first filter the signals using (1) and then resample all of the parameters in Table 1 to 5 Hz for synchronization.

We sorted the 12 patients who only receive NE as their vasopressor based on the quality, length, and availability of their data. Of the 103 patients, data from 91 patients were excluded. 31 patients were excluded due to lack of Norepinephrine dosage information and/or use of multiple vasopressor drugs during treatment. The other 60 are excluded due to having less than 24 hours of uninterrupted signals of MAP, ECG, and NE infusion rates or having ECG and ABP be substantially affected by a patient's physical movement. Therefore, the beat, systolic, and diastolic must detectable by the patient monitor system over 24 hours. Our study group consists of patients who receive NE as the vasopressor within 16-24 hours of ICU admission. We then take their first 10 hours of data to equalize the study time for each patient. The patients' characteristics are shown in Table 2 for reference. The baseline clinical information for all 12 patients is displayed in Table 2. The hemodynamic information is displayed in Table 3.

TABLE 2. Patient characteristics.

Characteristic	Central Tendency
Total Number of Patients	12
Age, years	62 (52-75)
Female sex	7 (58%)
Admission APACHE II score, points	24 (16.5-30)
28-day mortality	1 (8.3%)
Admission SOFA score, points	9.5 (8-12.5)
Admission systolic blood pressure, mmHg	92 (79-108)

Descriptive statistics organized by diagnostic group. Data reported as mean (SD), median (25%-75% interquartile range), or count (percentage of total).

B. DATA ANALYSIS AND VERIFICATION

We implement our algorithm in a way that will make it compatible with ultimate deployment in a real-time monitoring and control system. That is, we require no future data or extensive offline signal processing to make our predictions. We train our model with past data using (8) and then predict future MAP based on this model with (9). For each new data point, we repeat this process. Therefore, the algorithm creates and updates a patient-specific model in real-time to produce our predicted MAP minutes ahead of the actual measurement time. We then compare the predicted MAP with our observed MAP from patients. This verification process is also known as time series cross-validation [24].

In a second study, we sequentially removed inputs (the heart period, respiration wave, and/or norepinephrine) to study the contributions of each input to our model. For different combinations, we then study the average change in RMSE for each of the patients as a function of prediction intervals from 3.3 minutes to 20 minutes into the future.

C. CLINICAL CONTEXT

According to [4], MAP should be higher than 65 mmHg (i.e., the lower limit of the target MAP) to prevent a

TABLE 3. Patient hemodynamic data.

Patient ID	NE dosage (mg/(minkg)	MAP (mmHg)	SAP (mmHg)	DAP (mmHg)	Heart Interval (second/beat)
1	0.05 (0.024-0.054)	71 (64.7-77.5)	116 (105-127)	51 (44-56)	0.57 (0.43-0.69)
2	0.14 (0.13-0.17)	63 (58.9-66)	90 (84-96)	45 (41-48)	0.75 (0.72-0.78)
3	0.07 (0.04-0.1)	61 (57.2-64.1)	84 (79-90)	45 (42-48)	0.56 (0.55-0.59)
4	0.025 (0.02-0.03)	67 (64.5-72.4	110 (101-118)	53 (47-57)	0.69 (0.61-0.75)
5	0.03 (0.02-0.05)	65 (62.6-70)	104 (98-110)	50 (47-52)	0.62 (0.6-0.66)
6	0.2 (0.12-0.3)	70 (63-75)	122 (107-144)	47 (43-49)	0.75 (0.69-0.81)
7	0.06 (0.05-0.07)	68 (63.5-73.6)	98 (94-102)	54 (51-58)	0.66 (0.62-0.7)
8	0.017 (0-0.03	66 (64.5-72.6)	104 (95-112)	56 (50-61)	0.63 (0.58-0.67)
9	0.06 (0.03-0.09))	69 (65.2-73.4)	95 (88-104)	53 (49-58)	0.79 (0.72-0.86)
10	0.048 (0-0.05)	71 (65.9-73.4)	101 (95-107)	55 (51-59)	0.59 (0.55-0.64)
11	0.09 (0.04-0.15	65 (65.8-78.4)	103 (96-111)	53 (49-56)	0.56 (0.54-0.57)
12	0.07 (0-0.1)	69 (61.1-72.3)	106 (99-114)	48 (43-52)	0.68 (0.59-0.74)

Data reported as median (25%-75% interquartile range).

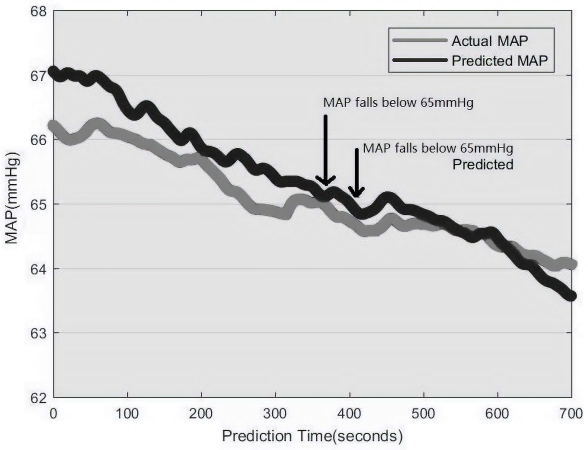

FIGURE 5. MAP hypotensive event 6 minutes prediction.

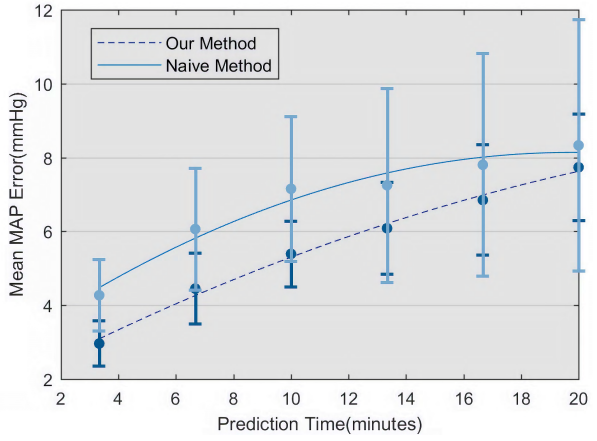

FIGURE 6. The mean error(RMSE) of the predicted MAP after training. The lines demonstrate the error of each individual patient. The vertical bars demonstrate the mean and 95% CI of them.

hypotensive event. Figure 5 shows an example of the MAP when dropping below 65 mmHg in one of our patients. The grey line represents the actual MAP that is collected from the patient while the black line represents the predicted MAP, calculated by using data from 6 minutes (360 seconds) prior. In the plot, the observed MAP drops below 65 mmHg at 360 seconds. The predicted MAP drops below 65 mmHg at 400 seconds (approximately one minute later). Therefore, we predict the drop below 65 mmHg at 40 seconds (i.e., when the MAP is approximately 67 mmHg).

Across our twelve patients, we observe a total of 11 hypotensive events (i.e., regions of time under 65 mmHg). We correctly predict 8 of those 11 events before their occurrence (predicting 6.67 minutes in the future). We also estimate the sensitivity, specificity, and accuracy of our predictions across all time. We consider the cases where we are predicting 3.33 minutes, 6.67 minutes, 10 minutes, 13.33 minutes, 16.67 minutes, and 20 minutes into the future. These results are shown in Table 4. As expected, the performance decreases as the prediction window increases, but we still achieve an 81% accuracy when predicting 10 minutes into the future.

IV. RESULTS AND DISCUSSION

The MAP-NE model demonstrates two results. First, we show that our method can successfully predict MAP better than a standard naive approach. Our naive approach assumes that the MAP does not change during the prediction interval. We also show that, as expected, the prediction error increases as the prediction interval increases.

Second, we show that incorporating NE infusion rate, or intermediary inputs between NE and MAP, improves our prediction efficiency. This demonstrates that we are predicting MAP based on the learned relationship between NE and MAP for each individual patient. This also suggests that the NE infusion can be tuned through our model to control MAP. We discuss each of these results in greater depth in this section.

Note our model is patient-specific and time-varying (i.e., adaptive). We perform a time-series cross-validation [24], which uses the data prior to the observed dataset as training data to forecast the future data. According to [24], overfitting is the same as failing to identify the correct model under these circumstances. Due to the patient-specific and time-varying nature of our model, there is no global model applied in our approach. In future work, we will also evaluate the use of a global model to improve the initial convergence efficiency for our personalized prediction model.

IEEE Journal of Translational Engineering in Health and Medicine

TABLE 4. Sample based hypotensive prediction accuracy.

Prediction time	3.33 mins	6.67 mins	10 min	13.33 mins	16.67 mins	20 mins
True Positive Rate (Sensitivity)	0.82	0.75	0.71	0.69	0.69	0.68
True Negative Rate (Specificity)	0.86	0.75	0.74	0.69	0.66	0.64
Accuracy	0.89	0.82	0.81	0.77	0.76	0.74

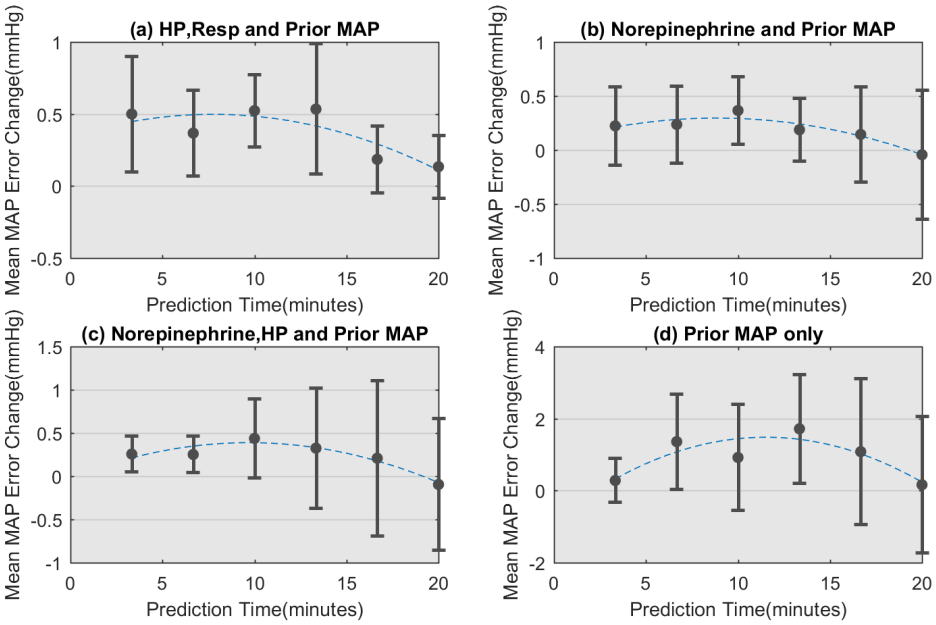

FIGURE 7. The mean MAP error change when naive method (top right), HP and Resp inputs(top left), NE and HP inputs (bottom right), and only NE applied(bottom right) compared with the results in Figure 5.

A. PRIMARY OUTCOME: PERFORMANCE VERSUS A NAIVE APPROACH

In this subsection, we verify the performance of our method through the data analysis study described in Section III. We learn $\mathbf{A}(n)$ from current and prior inputs, including the MAP. We then use this model to predict the future MAP. We measure the RMSE performance for an 8.8-hour window of patient data after the model has sufficient data to begin prediction (approximately 14 to 40 minutes).

Figure 6 demonstrates the RMSE for our method and the naive approach as a function of prediction time. The error bars illustrate a 95% confidence interval around the mean. For our approach, the mean error is 3 mmHg with a 3.33-minute prediction interval and 5.5 mmHg for a 10-minute prediction interval. This is compared with the respective mean errors of 4.5 mmHg and 7 mmHg for the naive approach. Hence, our approach has much tighter confidence intervals when compared with the naive method for all prediction times. Note that the error bars in Figure 6 illustrate the performance variability across all patients.

Overall, Figure 6 shows promising results. For 4 of 12 patients, the mean error remains under 5.5 mmHg for the entire prediction period. The best result exhibits a mean error of less than 3.5 mmHg for a 10-minute prediction interval and the worst result exhibits a mean error of approximately 9 mmHg for the 10-minute prediction interval. For longer prediction times, the errors expectedly converge as the prediction becomes increasingly more difficult. Our approach shows a statistically significant improvement (p-value < 0.04) for up to a 10-minute prediction interval.

Additionally, we applied the same data to conventional time-series prediction models, such as auto-regressive (AR) and auto-regressive moving average (ARMA), which act on only one time series input. With a MAP input and the same prediction lengths, ARMA was significantly computationally slower than our approach and often became unstable, leading to errors greater than 50 mmHg.

We also validated our approach with patients from the open MIMIC-III Waveform Database [25]. We restricted the validation to the nine patients within the MIMIC-III database that had all of the required concurrent data for the model. The MIMIC-III data yielded similar results, as shown in Table 5.

B. SECONDARY OUTCOME: INPUT VARIABILITY AND OTHERS

In this section, we illustrate our results with different inputs and illustrate how they affect our error. Figure 7 illustrates the additional RMSE error relative to the full input results after removing specific inputs. A positive value in Figure 7 indicates that the removed input has a positive contribution to the

TABLE 5. Sample based hypotensive prediction accuracy.

Prediction time	3.33 mins	6.67 mins	10 min	13.33 mins	16.67 mins	20 mins
MIMIC-III Data Mean Error (mmHg)	2.79	4.1	4.42	5.32	6.35	7.31
Our Data Mean Error (mmHg)	2.81	4.24	5.2	6.05	6.88	7.84

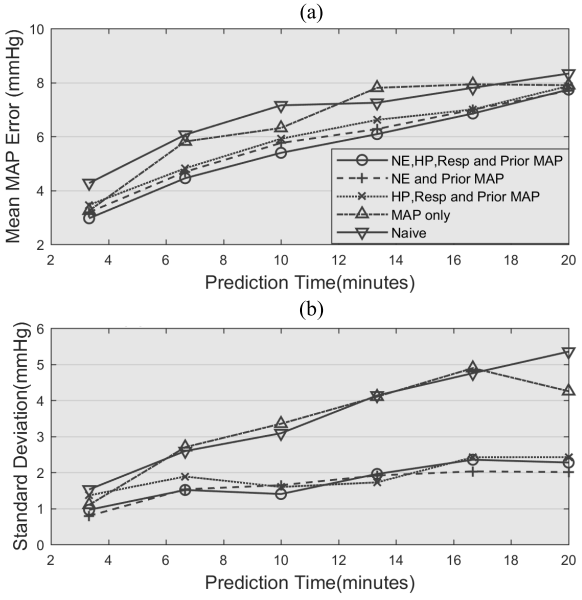

FIGURE 8. (a) The mean error of the predicted MAP after training. (b) The standard deviation of the mean error.

MAP estimate. The error bars illustrate the 95% confidence intervals.

Figure 7(a) shows the additional error exhibited after removing NE from the inputs. Removing NE increases the error by a statistically significant amount ($p < 0.04$) for up to a 13 minute prediction window. Note that the effect on MAP is relatively small since the effects of NE can still be indirectly related to Resp and HP. As the prediction length increases, the improvement from including NE decreases.

Figure 7(b) and Figure 7(c) show the change in RMSE when we remove HP and Resp as well as just remove Resp, respectively. While these results have similar trends, including HP helps reduce additional variation for short prediction times. The similarity between Figure 7(b) and Figure 7(c) is reasonable since MAP is primarily a function of prior MAP and NE while HP and Resp partially relate to the effects of NE with MAP.

Figure 7(d) shows the change in RMSE when only prior MAP is used as the input. In this result, the error and error variation increase significantly. As a result, prior MAP alone is a poor parameter for predicting future MAP, particularly for prediction intervals from 5 to 15 minutes.

Figure 8(a)-(b) illustrates the means and standard deviations for five different sets of inputs as a function of prediction time. Two observations can be derived from Figure 8. First, when NE is part of the input, the model accuracy improves and the standard deviation lowers. Second, if NE is not available, the combination of HP and Resp can function as a substitute since HP and Resp indirectly related to NE and MAP. However, including NE further improves the result, as shown in Figure 7(a).

V. CONCLUSION AND FUTURE WORK

This paper explores the topics of norepinephrine pharmacodynamics and MAP prediction on septic patients. There are few studies of MAP prediction in clinical settings. By reviewing the current understanding of the baroreflex system in human, we introduce a novel MAP model based on the NE infusion rate.

We then verified this model in a group of septic patients in an ICU. Our method was able to better predict MAP than a naive approach that assumed MAP was constant over a prediction interval. This improvement was statistically significant for up to a 10-minute prediction interval (p-value < 0.04). In addition, we demonstrated that incorporating NE as an input led to improvements in our result. This represents the first step toward a MAP control system based on NE infusion rates. With recent advances in machine learning [26], and deep neural networks with memory [27], incorporation of these techniques may improve our approach. We plan to investigate this in future efforts.

APPENDIX A
LIST OF SYMBOLS

- **MAP** – Mean arterial blood pressure;
- **HP** – Heart period;
- **NE** – Nor-epinephrine;
- **Resp** – Respiration;
- **LS** – Least squares;
- **PKPD** – Pharmacokinetic/Pharmacodynamic;
- **ANS** – Autonomic nervous system;
- **TPR** – Total peripheral resistance;
- **RMSE** – Root mean squared error;
- **RDE** – Research data export;

REFERENCES

[1] P. E. Marik and M. Mohedin, "The contrasting effects of dopamine and norepinephrine on systemic and splanchnic oxygen utilization in hyperdynamic sepsis," *Jama*, vol. 272, no. 17, pp. 1354–1357, 1994.

[2] R. Penrose, "A generalized inverse for matrices," *Math. Proc. Cambridge Phil. Soc.*, vol. 51, no. 3, pp. 406–413, 1955.

[3] M. Varpula, M. Tallgren, K. Saukkonen, L.-M. Voipio-Pulkki, and V. Pettilä, "Hemodynamic variables related to outcome in septic shock," *Intensive Care Med.*, vol. 31, no. 8, pp. 1066–1071, 2005.

[4] A. Rhodes *et al.*, "Surviving sepsis campaign: International guidelines for management of sepsis and septic shock: 2016," *Intensive Care Med.*, vol. 43, no. 3, pp. 304–377, 2017.

[5] P. T. Foteinou, S. E. Calvano, S. F. Lowry, and I. P. Androulakis, "A physiological model for autonomic heart rate regulation in human endotoxemia," *Shock*, vol. 35, no. 3, pp. 229–239, 2011.

[6] T. J. Mullen, M. L. Appel, R. Mukkamala, J. M. Mathias, and R. J. Cohen, "System identification of closed-loop cardiovascular control: Effects of posture and autonomic blockade," *Amer. J. Physiol.-Heart Circulatory Physiol.*, vol. 272, no. 1, pp. H448–H461, 1997.
[7] R. Mukkamala and R. J. Cohen, "A forward model-based validation of cardiovascular system identification," *Amer. J. Physiol.-Heart Circulatory Physiol.*, vol. 281, no. 6, pp. H2714–H2730, 2001.
[8] H. Beloeil, J.-X. Mazoit, D. Benhamou, and J. Duranteau, "Norepinephrine kinetics and dynamics in septic shock and trauma patients," *Brit. J. Anaesthesia*, vol. 95, no. 6, pp. 782–788, 2005.
[9] G. Eisenhofer, "The role of neuronal and extraneuronal plasma membrane transporters in the inactivation of peripheral catecholamines," *Pharmacol. Therapeutics*, vol. 91, no. 1, pp. 35–62, 2001.
[10] C. A. Chu, D. K. Sindelar, D. W. Neal, and A. D. Cherrington, "Hepatic and gut clearance of catecholamines in the conscious dog," *Metabolism*, vol. 48, no. 2, pp. 259–263, 1999.
[11] A. J. Johnston, L. A. Steiner, M. O'Connell, D. A. Chatfield, A. K. Gupta, and D. K. Menon, "Pharmacokinetics and pharmacodynamics of dopamine and norepinephrine in critically ill head-injured patients," *Intensive Care Med.*, vol. 30, no. 1, pp. 45–50, 2004.
[12] H. Kamendi *et al.*, "Quantitative pharmacokinetic–pharmacodynamic modelling of baclofen-mediated cardiovascular effects using BP and heart rate in rats," *Brit. J. Pharmacol.*, vol. 173, no. 19, pp. 2845–2858, 2016.
[13] B. Yapps *et al.*, "Hypotension in icu patients receiving vasopressor therapy," *Sci. Rep.*, vol. 7, no. 1, p. 8551, 2017.
[14] J. Zhu, X. Jin, R. Bighamian, C.-S. Kim, S. T. Shipley, and J.-O. Hahn, "Semiadaptive infusion control of medications with excitatory dose-dependent effects," *IEEE Trans. Control Syst. Technol.*, to be published.
[15] R. Bighamian, S. Soleymani, A. T. Reisner, I. Seri, and J.-O. Hahn, "Prediction of hemodynamic response to epinephrine via model-based system identification," *IEEE J. Biomed. Health Informat.*, vol. 20, no. 1, pp. 416–423, Jan. 2016.
[16] R. Bighamian, A. T. Reisner, and J.-O. Hahn, "An analytic tool for prediction of hemodynamic responses to vasopressors," *IEEE Trans. Biomed. Eng.*, vol. 61, no. 1, pp. 109–118, Jan. 2014.
[17] J. Lee and R. G. Mark, "An investigation of patterns in hemodynamic data indicative of impending hypotension in intensive care," *Biomed. Eng. Online*, vol. 9, no. 1, p. 62, 2010.
[18] M. Merouani *et al.*, "Norepinephrine weaning in septic shock patients by closed loop control based on fuzzy logic," *Critical Care*, vol. 12, no. 6, p. R155, 2008.
[19] P.-G. Guinot *et al.*, "Monitoring dynamic arterial elastance as a means of decreasing the duration of norepinephrine treatment in vasoplegic syndrome following cardiac surgery: A prospective, randomized trial," *Intensive Care Med.*, vol. 43, no. 5, pp. 643–651, 2017.
[20] P.-G. Guinot, E. Bernard, M. Levrard, H. Dupont, and E. Lorne, "Dynamic arterial elastance predicts mean arterial pressure decrease associated with decreasing norepinephrine dosage in septic shock," *Critical Care*, vol. 19, no. 1, p. 14, 2015.
[21] S. K. Mitra and Y. Kuo, *Digital Signal Processing: A Computer-Based Approach*, vol. 2. New York, NY, USA: McGraw-Hill, 2006.
[22] A. D. Back and A. C. Tsoi, "FIR and IIR synapses, a new neural network architecture for time series modeling," *Neural Comput.*, vol. 3, no. 3, pp. 375–385, 1991.
[23] J. Proakis, *Digital Communications* (Electrical Engineering Series). New York, NY, USA: McGraw-Hill, 2001.
[24] R. J. Hyndman and G. Athanasopoulos, *Forecasting: Principles and Practice*. Melbourne, VIC, Australia: OTexts, 2018.
[25] A. E. W. Johnson *et al.*, "MIMIC-III, a freely accessible critical care database," *Sci. Data*, vol. 3, May 2016, Art. no. 160035.
[26] M. Chen, Y. Hao, K. Hwang, L. Wang, and L. Wang, "Disease prediction by machine learning over big data from healthcare communities," *IEEE Access*, vol. 5, pp. 8869–8879, 2017.
[27] J. Y. Wang, L. Zhang, Q. Guo, and Z. Yi, "Recurrent neural networks with auxiliary memory units," *IEEE Trans. Neural Netw. Learn. Syst.*, vol. 29, no. 5, pp. 1652–1661, May 2018.